Lipid Domain Structure of the Plasma Membrane Revealed by Patching of Membrane Components

Thomas Harder, Peter Scheiffele, Paul Verkade, and Kai Simons

European Molecular Biology Laboratory, Cell Biology Programme, 69117 Heidelberg, Germany

Abstract. Lateral assemblies of glycolipids and cholesterol, "rafts," have been implicated to play a role in cellular processes like membrane sorting, signal transduction, and cell adhesion. We studied the structure of raft domains in the plasma membrane of non-polarized cells. Overexpressed plasma membrane markers were evenly distributed in the plasma membrane. We compared the patching behavior of pairs of raft markers (defined by insolubility in Triton X-100) with pairs of raft/non-raft markers. For this purpose we cross-linked glycosyl-phosphatidylinositol (GPI)-anchored proteins placental alkaline phosphatase (PLAP), Thy-1, influenza virus hemagglutinin (HA), and the raft lipid ganglioside GM1 using antibodies and/or cholera toxin. The patches of these raft markers overlapped extensively in BHK cells as well as in Jurkat T–lymphoma cells. Importantly, patches of GPI-anchored PLAP accumulated src-like protein tyrosine kinase fyn, which is thought to be anchored in the cytoplasmic leaflet of raft domains. In contrast patched raft components and patches of transferrin receptor as a non-raft marker were sharply separated. Taken together, our data strongly suggest that coalescence of cross-linked raft elements is mediated by their common lipid environments, whereas separation of raft and non-raft patches is caused by the immiscibility of different lipid phases. This view is supported by the finding that cholesterol depletion abrogated segregation. Our results are consistent with the view that raft domains in the plasma membrane of non-polarized cells are normally small and highly dispersed but that raft size can be modulated by oligomerization of raft components.

THE functional significance of lipid diversity in cell biological processes is now being unraveled. Recent developments show the involvement of specific lipids and lipid derivatives in membrane structure and dynamics. For example phosphoinositides have been shown to be important mediators of membrane–cytoskeleton interactions (Hirao et al., 1996) and vesicular transport. Additionally, there is evidence for a role of phosphatidic acid in the formation of specific coats mediating the formation of transport vesicles (Roth and Sternweis, 1997). Considerable attention has recently been drawn to lateral assemblies of glycosphingolipids and cholesterol (termed rafts), which have been proposed to form platforms for numerous cellular events including membrane trafficking, signaling, and cell adhesion.

Simons and Ikonen (1997) presented a model of glycosphingolipid–cholesterol rafts that predicts that attractive forces between sphingolipids with saturated hydrocarbon chains and cholesterol mediate the formation of lateral lipid assemblies in an unsaturated glycerophospholipid environment. The fundamental principle by which rafts exert their functions is a separation or concentration of specific membrane proteins and lipids in membrane microdomains. These domains may serve as platforms in the TGN for apical membrane sorting and as foci for recruitment and concentration of signaling molecules at the plasma membrane.

In polarized epithelial cells the apical and basolateral plasma membrane strongly differ in lipid and protein composition (Rodriguez-Boulan and Nelson, 1989). This lateral plasma membrane asymmetry is maintained by tight junctions which act as diffusion barriers. Membrane transport from the TGN to the apical or basolateral plasma membrane is mediated by distinct transport vesicles (Wandinger-Ness et al., 1990; Ikonen et al., 1995). Microdomains containing glycosphingolipid and cholesterol have been suggested to function as platforms for the generation of apically destined transport vesicles whereas specific signals in the cytosolic tails of transmembrane proteins confer basolateral targeting (Matter and Mellman, 1994; Simons and Ikonen, 1997). Cells that are not overtly polarized use similar separate apical and basolateral cognate routes to the cell surface (Müsch et al., 1996; Yoshimori et al., 1996). Whereas in epithelial cells rafts accumu-

T. Harder and P. Scheiffele contributed equally to this work.

Address all correspondence to K. Simons, Cell Biology and Biophysics Programme, European Molecular Biology Laboratory, Meyerhofstrasse 1, D-69012 Heidelberg, Germany. Tel.: (49) 6221 387 334. Fax: (49) 6221 387 512.

late at the apical surface, in fibroblasts basolateral and apical markers can freely mix after arrival at the cell surface. The organization of raft membrane domains within the plasma membrane of non-polarized cells is therefore a critical issue for understanding raft function.

The distribution of several raft markers including sphingolipids and glycosyl-phosphatidylinositol (GPI)[1]-anchored proteins has been analyzed on the surface of different non-epithelial cell types using immunoelectron microscopy (Mayor and Maxfield, 1995; Fujimoto, 1996). These markers where shown either to be evenly distributed over the plasma membrane or in case of the ganglioside GM1 in A431 cells to be slightly enriched in caveolae (Parton, 1994). Thus if raft domains are maintained in the plasma membrane of non-polarized cells they must be dispersed and highly dynamic and thus cannot be resolved by the microscopical techniques used (Harder and Simons, 1997).

One major tool currently used to study rafts is their relative resistance towards solubilization with Triton X-100 at 4°C. This leads to the isolation of a light membrane fraction termed detergent-insoluble glycolipid-enriched membranes (DIGs), which are thought to contain the remnants of the cellular raft domains aggregated together (Brown, 1992; Kurzchalia et al., 1995; Parton and Simons, 1995). Several membrane proteins are specifically enriched in the DIG fraction and thus considered to be raft proteins. These include a class of proteins that are anchored via a GPI moiety to the outer leaflet of the cellular membranes (Brown and Rose, 1992). Influenza virus hemagglutinin (HA) is a raft-associated transmembrane protein and its DIG association was shown to depend critically on amino acids in the transmembrane domain facing the outer leaflet of the bilayer (Scheiffele et al., 1997). Some cytoplasmic proteins are found in the DIG fraction and are thus thought to be associated to raft domains via the cytoplasmic leaflet of the lipid bilayer. These include several signaling molecules such as Gα subunits of heterotrimeric G proteins or the src-like protein tyrosine kinases lck, fyn, and lyn that depend on multiple acylation for DIG association (Rodgers et al., 1994; Shenoy-Scaria et al., 1994; Mumby, 1997; Wolven et al., 1997).

Triton X-100 insolubility has proven a useful starting point for the analysis of raft domains and several lines of evidence indicate the validity of this criterion. Depletion of sphingolipids or cholesterol abolish the association of several proteins with the DIG fraction as predicted from their involvement in the formation of lateral lipid assemblies (Cerneus et al., 1993; Hanada et al., 1995; Scheiffele et al., 1997). Further support comes from the observation that HA as well as GPI-anchored placental alkaline phosphatase (PLAP) become DIG associated upon biosynthetic transport indicating their incorporation into rafts after entering the Golgi complex (Skibbens et al., 1989; Brown and Rose, 1992). Moreover reconstitution experiments of GPI-anchored PLAP into liposomes of different lipid composition showed that the Triton X-100 insolubility of PLAP critically depends on a raft lipid environment (Schroeder et al., 1994). Recently a tight correlation between detergent insolubility and the formation of a liquid-ordered phase by sphingolipids and cholesterol in a liquid crystalline lipid bilayer could be demonstrated (Ahmed et al., 1997).

Nevertheless the characterization of raft domains using Triton X-100 insolubility has its limitations. DIGs will not represent the actual organization of rafts in cellular membranes as raft markers were shown to coalesce upon extraction with Triton X-100 (Mayor and Maxfield, 1995). A further problem is that raft affinities of different markers are difficult to characterize. It is possible that relatively weak interactions with raft lipids cannot be detected using DIG association. Moreover, differential extraction does not demonstrate that the specific attraction between lipids and between lipids and proteins are responsible for the formation of raft domains. Here we used a different approach to study these interactions. We examined membrane proteins and lipids cross-linked with antibodies or toxins. Based on copatching behavior of different membrane components, our data revealed attractive or repellant forces between clusters of different membrane proteins and lipids. Our data provide evidence for specific lipid–lipid and lipid–protein interactions in cell membranes governing raft dispersion and clustering.

Materials and Methods

Cells

BHK-21 cells were maintained at 37°C in 5% CO_2 in a humidified atmosphere in G-MEM (GIBCO BRL, Gaithersburg, MD), 5% FCS, 10% tryptose phosphate (GIBCO BRL), supplemented with penicillin (100 U/ml)/streptomycin (100 μg/ml) and 2 mM glutamine (all GIBCO BRL). 2B2318 T–hybridoma cells (Blackman et al., 1992) as well as Jurkat T–lymphoma line (American Type Culture Collection, Rockville, MD) were kept in RPMI 1640 medium (GIBCO BRL), 10% FCS, penicillin (100 U/ml)/streptomycin (100 mg/ml), 2 mM glutamine at 37°C in 5% CO_2 in a humidified atmosphere.

Antibodies and Expression Constructs

Monoclonal mouse and polyclonal rabbit anti-PLAP antibodies were obtained from Dako (Glostrup, Denmark), anti–human transferrin receptor (hTfR) mAb from Boehringer Mannheim (Mannheim, Germany), anti–Thy-1 monoclonal antibody from Serotec Ltd. (Oxford, UK), and the rabbit antibody against human transferrin from Zymed Labs Inc. (South San Francisco, CA). Anti-HA (japan-strain A/Japan/305/57) rabbit serum No. 1 was a gift from M. Roth (University of Texas, Dallas, TX). Anti-HA (japan-strain A/Japan/305/57) rabbit serum No. 2 was generated in our laboratory using a preparation of viral membrane proteins in micelles as antigen (Scheiffele et al., 1997). Affinity-purified anti–vesicular stomatitis virus glycoprotein (VSV-G) was prepared in our laboratory. Anti–low density lipoprotein receptor (LDL-R) mAb C7 was a gift from K. Matter (University of Geneva, Geneva, Switzerland). Anti–human *fyn* polyclonal antibodies were obtained from G. Alonso (European Molecular Biology Laboratory [EMBL], Heidelberg, Germany). Preabsorbed secondary FITC goat anti–rabbit or rhodamine goat anti–mouse antibodies, as well as 6-nm colloidal gold goat anti–mouse and 12-nm gold goat anti–rabbit were from Dianova (Hamburg, Germany).

A PLAP expression construct driven by Rous sarcoma virus (RSV) promoter was obtained from D. Brown (State University of New York, Stony Brook, NY; Brown et al., 1989), pSG-5 expression construct for human fyn driven by SV-40 early promoter was obtained from G. Alonso. All of the following expression constructs use the cytomegalovirus (CMV) promoter. The hTfR expression construct in pCMV5 was described previ-

1. *Abbreviations used in this paper*: CTx, choleratoxin B subunit; DIGs, detergent-insoluble glycolipid-enriched complexes; GM1, ganglioside GM1; GPI, glycosyl-phosphatidylinositol; HA, hemagglutinin; hTfR, human transferrin receptor; LDL-R, low density lipoprotein receptor; PC, phosphatidylcholine; PLAP, placental alkaline phosphatase; VSV-G, vesicular stomatitis virus glycoprotein.

ously (Harder and Gerke, 1993). A hTfR deletion mutant (hTfR del 5–41) lacking amino acids 5–41 that deletes the basolateral targeting as well as the endocytosis signal (Odorizzi and Trowbridge, 1997) was constructed by PCR using the oligonucleotide 5′-TCCTGGGATCCCAGAATG-ATGGATCAAGCTGTAGATGAAGAAG-3′ and the oligonucleotide 5′-CTACGGAATTCTTACTTACCCAGGCGGTTCATTTCGATATCA-GTGTAAAACTCATTGTCAATGTCCC-3′ in a PCR reaction with the hTfR wild-type cDNA as template. The resulting product was cloned as a EcoRI–BamHI fragment into pcDNA3 (Invitrogen, Carlsbad, CA). HA wild type (japan-strain A/Japan/305/57) was cloned as a HindIII–BamHI fragment into pcDNA3 (Invitrogen), pCB6 HA Y543 expression construct and wild-type HA cDNA were obtained from M. Roth. HA-tail minus was constructed using HA wild-type cloned into pcDNA3 as a substrate for a PCR reaction using T7 primer (Pharmacia Biotechnology, Inc., Piscataway, NJ) and the oligonucleotide 5′-CTACATCCAGAAA-GAGATCCCAGC-3′, and then cloned into pcDNA3. This introduced a stop codon at amino acid 536, immediately after the transmembrane region of HA, thus deleting the complete cytoplasmic tail region. The LDL-R constructs LDL YA-18 and LDL YY-A18A35 in pCB6 were obtained from K. Matter (Matter et al., 1992). All plasmids were purified using Quiagen columns (Quiagen, Inc., Chatsworth, CA) according to the manufacturer's instruction.

Transfection and Viral Infection

1/300 (or 1/200 for biochemical experiments) from a confluent BHK cell 75-cm^2 tissue culture flask (Nalge; Nunc Inc., Naperville, IL) were seeded in 2 ml of full medium on glass coverslips for immunofluorescence or Thermanox coverslips (Nunc Inc.), for electron microscopy in 3-cm tissue culture dishes. Per dish, 1–2 μg of each expression plasmid was used for cotransfection. Transfections were performed in Opti-MEM (GIBCO BRL) with 2–4 μl of lipofectamine (GIBCO BRL) according to the instructions of the manufacturer. The DNA/lipofectamine was kept on the cells for 4 h. 5×10^5 Jurkat T–lymphoma cells suspended in 1 ml Opti-MEM were transfected for 4 h using 4 μl of lipofectamine and 2 μg of plasmid DNA in Falcon 15-ml polystyrene tubes (Becton Dickinson labware, Franklin Lakes, NJ). Cells were collected before and after transfection by centrifugation at 800 rpm in a Megafuge 1.0 centrifuge (Heraeus Sepatech, Hanau, Germany) for 5 min. The transfected cells were analyzed after 16 h incubation at 37°C in full medium.

For infection with VSV, cells were washed with PBS and virus adsorption was performed for 1 h at 37°C in Infection medium (MEM, 50 mM Hepes, pH 7.3, penicillin (100 U/ml)/streptomycin (100 μg/ml), 0.2% BSA) using 20 pfu/cell. Infection was allowed to continue for 1 h and VSV-G was chased to the surface with a cycloheximide block (5 μg/ml) for 1 h.

Immunofluorescence and Antibody-induced Patching

For immunofluorescence, cells were fixed for 4 min in 3.7% formaldehyde in PBS at 8°C and subsequent incubation in methanol at −20°C for 5 min (Osborn et al., 1988). The fixed cells were incubated for 1 h at 37°C with the respective dilution of the antibodies in PBS, 2 mg/ml BSA (PBS/BSA), and washed three times for 3 min at room temperature in PBS/BSA followed by incubation with the respective secondary antibodies for 1 h at 37°C. After washing, the cells were mounted in 20 mM Tris HCl, pH 8.0, 80% glycerol, 4% (wt/vol) *N*-propyl gallate as anti-fade.

For the patching experiments antibodies were dialyzed against PBS (except the colloidal gold–labeled antibodies). Dilutions were made in MEM, 50 mM Hepes, pH 7.3, 2 mg/ml BSA. The monoclonal as well as the polyclonal antibody against PLAP were diluted 1:35. Anti-HA serum No. 1 was preabsorbed against nontransfected BHK cells and used 1:20. Anti-HA serum No. 2 was used at 1:200. Mouse mAb against LDL-R was used as 1× tissue culture supernatant, anti–VSV-G affinity-purified antiserum at 1:200, anti-transferrin rabbit polyclonal at 1:100, anti-hTfR monoclonal at 1:100. Cells were incubated for 1 h at 12°C with the respective combination of antibodies, and then washed briefly at 4°C in PBS/BSA. Further cross-linking with secondary antibodies was performed at 12°C for 1 h. Either 1:100 dilution of the mixed fluorescence-labeled secondary or 1:20 of the colloidal gold secondary antibodies were used. In some experiments, the incubation with primary and secondary antibodies were performed at 37°C twice for 20 min. For fluorescence, cells were fixed and mounted as described above. Pictures exhibiting easily recognizable patches of the two respective markers were taken on an Axiophot microscope (Carl Zeiss, Oberkochen, Germany) coupled to a Colour Coolview 8-bit CCD color camera (Photonic Science, Millham, UK). Filter settings for simultaneous detection of FITC and rhodamine signals were used. The digital images were processed using Photoshop software (Adobe Systems, Inc., Mountain View, CA) on a Macintosh computer (Apple Computer Co., Cupertino, CA). For better visualization, images showing a single color channel were transferred to a gray scale. We ensured that the linear signal intensities detected for both fluorophors were covered by a linear scale of the pixel intensities. Pictures were taken focusing on the apex of the cells. Under these conditions, fluorescence signal from the ventral side of the cells was not detected.

For electron microscopy, colloidal gold–labeled cells on Thermanox plastic coverslips were fixed in 2.5% glutaraldehyde (Serva, Heidelberg, Germany) in 100 mM cacodylate buffer, pH 7.35, for 30 min at room temperature, thoroughly rinsed in tri-distilled water incubated with 4% OsO_4 for 30 min, rinsed again, and then incubated in 3% uranyl acetate. After gradual dehydration in ethanol the coverslips were embedded in Epon. After removing the coverslips, ultrathin (50–70 nm) sections were counterstained in 3% uranyl acetate for 5 min, Reynold's lead citrate for 1 min, and then analyzed on a 10-C electron microscope (Carl Zeiss). Cholesterol extraction was performed as described (Klein et al., 1995; Keller and Simons, 1998*a*). Briefly, BHK cells were extracted with 10 mM methyl-β-cyclodextrin (Sigma Chemical Co.) in MEM, 50 mM Hepes, pH 7.3, 0.35 g/liter carbonate (low carbonate) at 37°C on a rocking platform for 1 h, and subsequently processed as described above.

Quantitation of Copatching

The expression levels of the two transiently expressed markers varied from cell to cell on one coverslip. This and the differences in cell shape precluded a computer-based quantitation of the copatching. For quantitative analysis images of 20 randomly selected cells expressing each pair of markers were stored as digital files in a coded form. By inspection the images were scored in a blinded fashion by an individual not involved in the recording into four categories of copatching/segregation: (*1*) coclustering (>80% overlap); (*2*) partial coclustering (clearly coinciding spots); (*3*) random distribution; and (*4*) segregation. Only areas of the cells that were in focus were considered for quantitation. The percentage of cells falling into the respective categories in at least four independent experiments (each performed in parallel) were expressed as average ± SD, thus ensuring objectivity and reproducibility of the scoring.

Choleratoxin–FITC Labeling of GM1 Labeling

Jurkat cells were transfected with PLAP and hTfR del 5–41 expression constructs as described above. Copatching of GM1 with PLAP and hTfR del 5–41 was performed by simultaneous incubation in suspension (in 500 μl MEM, 2 mg/ml BSA per 5×10^5 cells) at 12°C with the anti-PLAP or hTfR mAb and FITC–choleratoxin B subunit (FITC-CTx; Sigma Chemical Co.) (8 μg/ml) under gentle rocking. Subsequently, primary antibodies were further clustered with rhodamine anti–mouse antibodies. Cells were collected, washed before and between incubations by centrifugation at 2,000 rpm in a tabletop centrifuge (Eppendorf, Hamburg, Germany) at 4°C, and then suspending in 1 ml PBS/BSA. Cells were attached to polylysine (5 mg/ml; Sigma Chemical Co.), coated microscope slides, fixed, and then mounted as described above. 2B2318 T–hybridoma cells were incubated with anti–Thy-1 mAb and FITC-CTx followed by rhodamine anti–mouse antibodies as described above for the Jurkat cells.

Flotation Gradients

BHK cells on 3-cm dishes expressing PLAP were used 16 h after transfection. In parallel, untransfected cells in 3-cm culture dishes were infected with VSV for 1 h followed by a 2-h incubation at 37°C with a chase of cycloheximide during the last hour. Cells were washed in PBS, and VSV-G and PLAP were clustered as described above using affinity-purified, anti–VSV-G and anti-PLAP mAbs, followed by incubation with the respective secondary antibodies. Cells were washed twice in ice-cold PBS before, between, and after the incubations. Cells were scraped in PBS and spun down at 2,000 rpm 4°C in an tabletop centrifuge (Eppendorf). The cells were subsequently lysed in 200 μl TNE (25 mM Tris HCl, pH 7.4, 150 mM NaCl, 5 mM EDTA, 1 mM DTT, CLAP protease inhibitor cocktail), 10% sucrose, 2% Triton X-100 at 4° or 30°C, respectively. The cell pellet was resuspended thoroughly by pipetting through a 200-μl yellow pipetting tip and incubated for 20 min on ice or 30°C, respectively, and then mixed again after 10 min with 400 μl of cold 60% Optiprep™ (Nycomed-Pharma, Oslo, Norway) was added to the extract and the mix was transferred to an SW60 centrifuge tube (Beckman, München, Germany). The

sample was overlaid with a 600-μl step of each of 35%, 30%, 25%, 20%, 0% Optiprep™ in TNE, 10% sucrose, 2% Triton X-100. The gradients were spun for 4 h, at 40,000 rpm at 4°C. Six fractions from the top of the gradient were collected. The fractions were TCA precipitated and analyzed by Western blot with anti–VSV-G mAb P5D4 (Kreis, 1986) and anti-PLAP rabbit polyclonal antibodies followed by HRP-coupled secondary antibodies (Bio-Rad Laboratories) and ECL (Amersham Buchler GmbH, Braunschweig, Germany).

Results

Extracellularly exposed lipids and membrane proteins can be laterally cross-linked with specific antibodies or multivalent bacterial toxins. This causes a redistribution of these plasma membrane elements which tend to form patches on the cell surface (Spiegel et al., 1984). Here we studied the patching behavior of different proteins and lipids. We focused specifically on putative glycosphingolipid–cholesterol raft elements and compared their behavior to membrane components presumed to have low affinity for raft domains. The starting point to define raft-associated proteins and lipids was their association to the Triton X-100–insoluble DIG membrane fraction. Our aim was to analyze how raft and non-raft domains are organized in the plasma membrane.

For this purpose we compared the patching behavior of pairs of either two raft membrane proteins or a raft protein and non-raft protein in fibroblastoid BHK 21 cells. We then used fluorescence-labeled choleratoxin to visualize and patch the raft-associated ganglioside GM1. The cells were incubated at low temperatures with a mouse mAb against one protein and a rabbit polyclonal antibody against the other protein marker followed by the two different fluorescence- or colloidal gold–labeled secondary antibodies. The relative distribution of the patches of the two different markers could then be analyzed using immunofluorescence or electron microscopy, respectively.

Copatching of Influenza HA and GPI-anchored PLAP

We expressed as raft-associated protein markers the trimeric transmembrane protein influenza hemagglutinin (HA) and the GPI-anchored dimeric protein placental alkaline phosphatase (PLAP). A well-characterized artifact when studying the distribution of a GPI anchored on the cell surface proteins is the antibody-induced redistribution of these proteins into patches if the proteins are not properly cross-linked by the fixative (Mayor et al., 1994). In our hands, paraformaldehyde fixation protocols resulted in varying degrees of patching of PLAP (data not shown). We obtained reproducible results using a fixation protocol using brief formaldehyde fixation and subsequent incubation in methanol at −20°C (FA/MeOH-fixation; Osborn et al., 1988). In cotransfected BHK cells, both markers were then evenly distributed over the plasma membrane (Fig. 1, *A–C*). Thus this fixation procedure produces the dispersed patterns of distribution published for other GPI-anchored proteins in line with previous detailed studies that showed no indication for clustering of GPI-anchored proteins on the cell surface of mammalian cells (Mayor and Maxfield, 1995). In cotransfected BHK cells, both markers were evenly distributed over the plasma membrane (Fig. 1, *A–C*). This is in line with previous detailed studies that showed no indication for clustering of GPI-anchored proteins on the cell surface of mammalian cells (Mayor and Maxfield, 1995). The additional intracellular staining derived from Golgi and/or endosomal localization of the overexpressed proteins. For an immunofluorescence analysis of antibody-induced cross-linking, we simultaneously incubated the cells with an anti-PLAP mAb, and either one of two different polyclonal rabbit sera against influenza virus HA. This incubation was performed at 12°C, thus minimizing metabolic activity of the cells during the incubations (transferrin is not internalized under these conditions; data not shown). This was followed by an incubation with the respective FITC- and rhodamine-coupled secondary antibodies at 12°C. Microscopical inspection of the fluorescence signal showed redistribution of both markers into patches. These patches overlapped in closely coinciding patches showing that the patches of the independently cross-linked markers coalesce (Fig. 1, *D–J*). The extensive overlap of the two cross-linked raft markers shows that there exist attractive forces between the independently formed patches of PLAP and HA. We then analyzed whether attractions between the independently cross-linked raft markers can still be detected when the cells are incubated at 37°C. We performed the patching experiments at 37°C with short antibody incubations (20 min for each the primary and the secondary antibodies, respectively). Endocytosis of PLAP and HA during these incubation time is <5% (Verkade, P., and T. Harder, unpublished results). We observed that the cross-linked PLAP and HA copatch at the surface of the BHK cells (Fig. 1, *K–M*) although not as extensively as at 12°C and the patches were often larger in size. These differences are possibly due to shorter incubation times used and cellular responses to the patching of the membrane components. Nevertheless, this shows that the forces responsible for copatching are not only detectable at 12°C but exist under physiological temperatures.

To determine the properties of the HA molecules that are responsible for these attractive forces we analyzed the coclustering of mutants of the HA molecule. We used a mutant of HA where the cytoplasmic tail was deleted (HAΔT). Here, as with the wild-type HA, an extensive overlap of HAΔT and PLAP was apparent (Fig. 1, *N–P*) showing that copatching is not determined by a direct interaction between HA and cytosolic components. We then tested the HA mutant in which cysteine 543 is mutated to tyrosine (HA Y543). This variant of HA contains a basolateral targeting signal and is efficiently internalized via clathrin-coated pits (Lazarovits and Roth, 1988; Brewer and Roth, 1991). HA Y543 copatched with GPI-anchored PLAP after antibody-induced cross-linking to the same extent as wild-type HA (Fig. 1, *R–T*) showing that a basolateral targeting signal and the potential to interact with a clathrin lattice does not perturb the interactions responsible for the copatching.

Segregation of Clustered PLAP from Patches of Transferrin Receptor and LDL Receptor

To analyze whether a common preference for raft lipid environment mediates the tight association of the cross-linked HA and PLAP we cross-linked membrane proteins not associating to DIGs. We tested copatching of the wild-

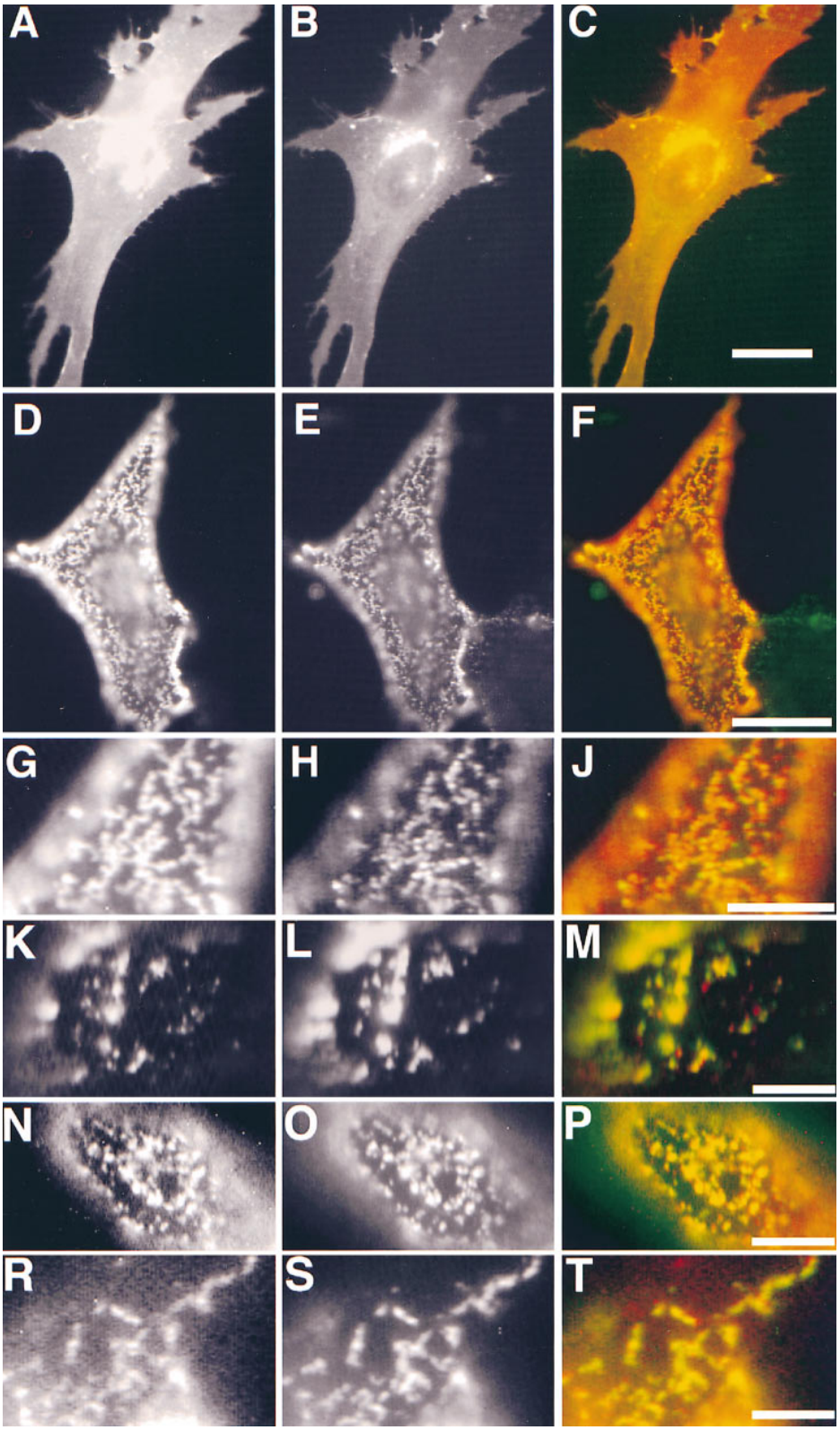

Figure 1. Copatching of cross-linked PLAP with influenza HA. The left column shows PLAP distribution in different experiments, the middle column HA distribution, and the right column the merge of the two signals. (*A–C*) Immunofluorescence of PLAP and wild-type HA on fixed BHK cells. (*D–M*) Copatching of PLAP with HA wild type. *G–J* show a detail of *D–F*. *K–M* show the copatching of PLAP and HA at 37°C. (*N–P*) Copatching of PLAP with HA tail minus, and (*R–T*) HA 543Y. PLAP antibodies were detected using rhodamine anti–mouse (*red*), HA antibodies using FITC anti–rabbit-labeled (*green*) secondary antibodies. Bars: (*C*) 10 μm; (*F*) 5 μm; (*J*, *M*, *P*, and *T*) 3 μm.

type hTfR, the LDL-R, and VSV-G in patching experiments with PLAP. Together with PLAP we transiently expressed hTfR and the LDL-R in BHK cells. Immunofluorescence on FA/MeOH-fixed cells showed that the hTfR and PLAP expression generated a strong staining that appeared evenly distributed over the whole plasma membrane (Fig. 2, *A–C*). We did not detect a concentration of the hTfR in coated pits most probably because the clathrin-dependent internalization pathway is saturated by the high number of receptors in the plasma membrane (Warren et al., 1997). Intracellular staining derives from Golgi and endosomal localization of the overexpressed markers. We then fol-

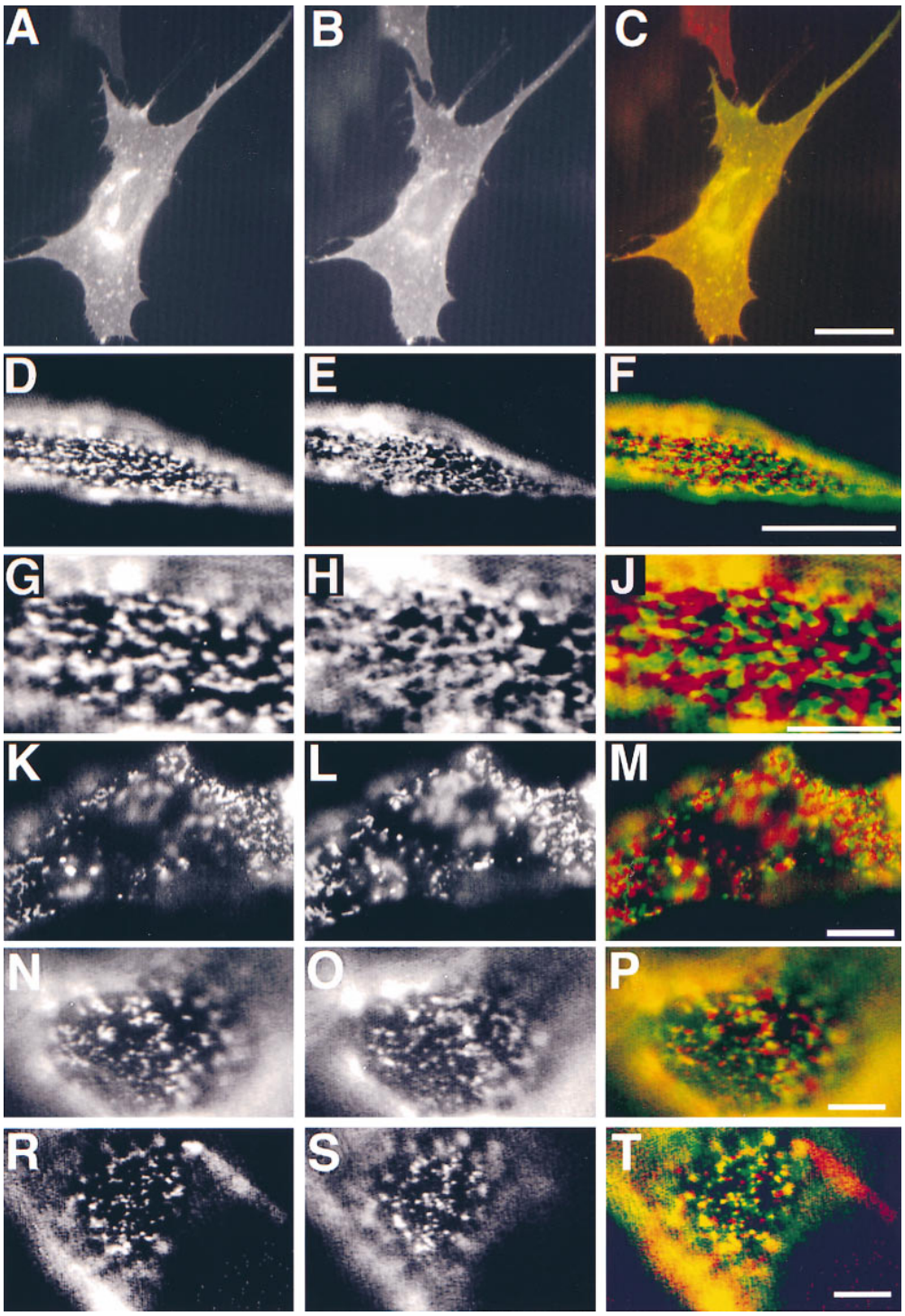

Figure 2. Patching of PLAP and transmembrane proteins hTfR, hTfR del 5–41, LDL-R YA18, and VSV-G. The left column shows PLAP distribution. The middle column shows distribution of hTfR (*B*, *E*, *H*, and *L*), LDL-R YA 18 mutant (*O*), and VSV-G (*S*). The right column shows the merge of the two signals. *A–C* shows immunofluorescence of PLAP (*green*) and hTfR (*red*) on fixed BHK cells. *D–J* shows segregation of patched PLAP (*green*) and hTfR (*red*). *G–J* shows a detail of *D–F*. *K–M* shows segregation patches of cross-linked PLAP (*green*) and hTfR del 5–41 (*red*) at 37°C. *N–P* shows patches of cross-linked PLAP (*green*) and LDL-R YA18 (*red*). *R–T* show patches of PLAP (*red*) and VSV-G (*green*). Bars: (*C*) 10 μm; (*F*) 5 μm; (*J*, *M*, *P*, and *T*) 3 μm.

lowed the behavior of cross-linked markers. Antibody-induced cross-linking of hTfR alone by incubation with a mouse mAb and respective secondary antibodies caused the formation of patches (data not shown). If PLAP was simultaneously cross-linked with hTfR using a polyclonal rabbit antibody, the patches of the respective markers were separated from patched PLAP (Fig. 2, *D–J*). In cells expressing high amounts of both markers this lead to a mosaic staining covering the complete cell surface. Importantly, the same results were obtained when a transferrin polyclonal antibody was used in conjunction with a mouse anti-PLAP mAb to induce simultaneous cross-linking of hTfR and PLAP (data not shown). Therefore segregation of the hTfR and PLAP patches was independent from the antibody combination used. These data clearly show that the attractive forces between cross-linked HA and PLAP molecules are not detectable between patches of hTfR and PLAP.

To rule out the possibility that interaction with clathrin-coated pits is responsible for the segregation, we constructed a mutant of hTfR where the cytosolic amino acids 5–41 are deleted (hTfR del 5–41). This deletion destroys basolateral targeting and renders the receptor incapable of

interacting with clathrin-coated pits (Odorizzi and Trowbridge, 1997). We observed that patches of hTfR del 5–41 were clearly segregated from cross-linked PLAP (data not shown). Moreover, this mutant allowed us to test whether patched TfR and PLAP still segregate at 37°C. We performed patching in cells coexpressing hTfR del 5–41 and PLAP at 37°C. The incubation times were 20 min for the primary antibody and secondary antibody, respectively. Under these conditions patches of PLAP and hTfR del 5–41 were sharply separated at the surface of the BHK cells (Fig. 2, *K–M*) showing that segregation of hTfR and PLAP can be detected at physiological temperatures.

We then tested LDL-R in the patching experiments together with PLAP. We expressed two mutants of the LDL-R. In the first mutant YA 18 the signal for coated pit localization—overlapping with the distal basolateral localization signal—is destroyed. The second mutant, YYA18A35, has lost both basolateral targeting signals and clathrin-coated pit localization signal and is transported apically in MDCK cells (Matter et al., 1992). We used a mouse mAb against LDL-R and a polyclonal anti-PLAP antibody followed by the respective fluorescently labeled secondary antibodies to compare the patches of LDL-R and PLAP. In both mutants there was little overlap visible (Fig. 2, *N–P*; and data not shown). However, in some cells clearly coinciding spots could be detected. We performed a quantitative analysis of the relative overlap of patched PLAP and the LDL-R YA 18 variant. 20 randomly taken fluorescence images of PLAP patched together with HA, VSV-G (see below), LDL-R YA 18, and hTfR were stored as coded digital files. The images were scored into four categories by an individual not involved in the recording of the pictures: (*1*) coclustering (>80% overlap); (*2*) partial coclustering (clearly coinciding spots); (*3*) random distribution; and (*4*) segregation. The percentages of cells falling into the four different categories are shown as averages from four independent experiments (Fig. 3). The objectivity and reproducibility of the scoring is indicated by the relatively low variation of the scores for every pair of markers. This analysis showed that patches of LDL-R and PLAP did not exhibit the extensive overlap seen for HA and PLAP clusters, nor were they as sharply separated as patches of hTfR and PLAP.

We then tested the VSV-G protein, which is also soluble in Triton X-100. As none of the expression constructs (including those that gave good expression in HeLa cells) resulted in efficient VSV-G expression in our BHK 21 cell system we infected PLAP expressing BHK cells with vesicular stomatitis virus. VSV-G and PLAP were clustered with a rabbit polyclonal antibody and a mouse mAb, respectively. We observed partial coclustering (Fig. 2, *R–T*). Quantification showed that copatching was intermediate between that observed for HA and PLAP and that of LDL-R and PLAP, respectively (Fig. 3).

Taken together we observed that different membrane proteins exhibit different degrees of copatching with PLAP ranging from a high degree of copatching of HA to a complete segregation in case of hTfR.

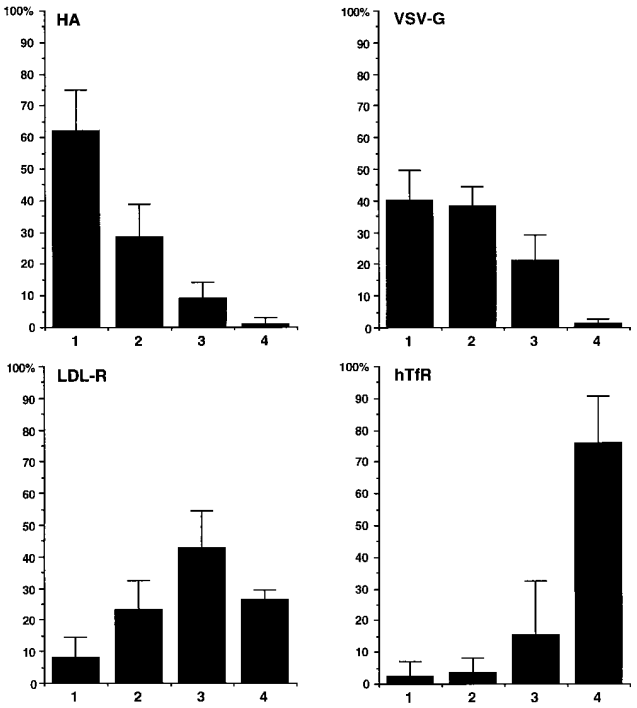

Figure 3. Quantitation of copatching of influenza HA, VSV-G, LDL-R, and hTfR with cross-linked PLAP. Patches of the different membrane markers were scored into four categories: (*1*) copatching (>80% overlap); (*2*) partial copatching (clearly overlapping regions); (*3*) random distribution; (*4*) segregation. The percentages of cells falling into each category are expressed as averages and SD from at least four experiments.

Involvement of Glycosphingolipids and Cholesterol

If HA and PLAP copatching is mediated by a common raft lipid preference raft lipids are predicted to copatch with PLAP. Glycosphingolipids are considered to be major constituents of raft domains because of their strong enrichment in the DIG membrane fraction. We therefore analyzed the patching behavior of the ganglioside GM1. GM1 was detected and clustered together with PLAP and hTfR del 5–41 using FITC-CTx as a specific clustering agent. Importantly, cholera toxin is pentavalent for GM1 thus causing the formation of clusters of five GM1 molecules, but not of large GM1 lattices (Merrit et al., 1994). BHK cells contain too low amounts of GM1 to be detected in our experiments. We therefore used Jurkat cells transiently expressing PLAP and hTfR del 5–41. Binding of FITC-CTx to these cells was performed during the incubation with the primary antibodies against PLAP and hTfR. By fluorescence microscopy the FITC-CTx/GM1 patches could be compared with the rhodamine signal of the secondary antibodies used to cross-link the anti-PLAP antibodies. This analysis showed an extensive overlap between the antibody-induced patches of PLAP and the patches of ganglioside GM1 induced by CTx (Fig. 4, *A–C*). These data clearly show that the cross-linked glycosphingolipids copatch with PLAP supporting a specific involvement of lipid interactions in the copatching phenomenon.

Importantly, in the control experiments clustered hTfR del 5–41 is excluded from patches of CTx–cross-linked GM1 showing again that hTfR clusters are segregated from the lipid domains of patched GM1 (Fig. 4, *D–F*). This strengthens the view that a distinct lipid environment of hTfR patches and PLAP/GM1 causes their separation.

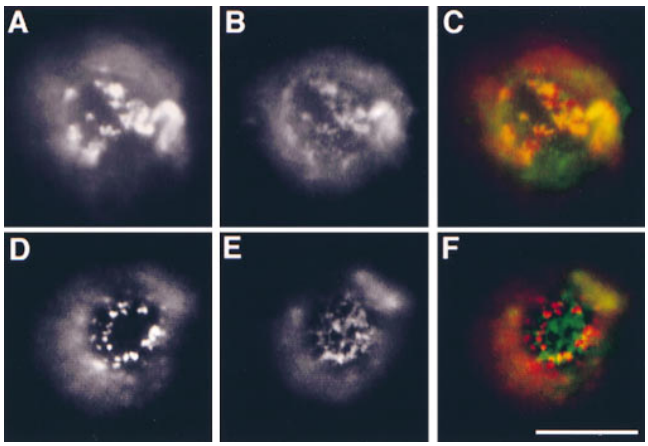

Figure 4. Patching of GM1/cholera toxin with PLAP and hTfR del 5–41 in Jurkat T–lymphoma cells. FITC-CTx conjugate was used to patch and stain GM 1 (*green*). Respective mAbs against PLAP or hTfR were used followed by incubation with rhodamine-coupled secondary antibodies (*red*). PLAP (*A*) and GM1 (*B*) show extensive copatching (merge in *C*). Patched hTfR del 5–41 (*D*) and GM1 patches (*E*) are largely exclusive (merge in *F*). Bar, 5 μm.

We also tested whether of cholesterol depletion has an effect on the patching behavior. Cholesterol was extracted from the cells using methyl-β-cyclodextrin, a cyclic sugar with a hydrophobic cavity that specifically binds cholesterol rendering it soluble in aqueous solution (Klein et al., 1995). (See Keller and Simons, [1998*a*] for detailed characterization of cholesterol depletion in BHK cells.) This procedure has been shown extract ~70% of cellular cholesterol from BHK cells (Keller and Simons, 1998*a*) and to abolish association of several raft proteins with the Triton X-100–insoluble membranes indicating a weakening of interactions with raft domains (Scheiffele et al., 1997). We followed the patching behavior of PLAP (Fig. 5 *A*) as well as hTfR (Fig. 5 *B*) in methyl-β-cyclodextrin extracted cells. Indeed in comparison to control cells the clusters of PLAP in the cholesterol-depleted cells were much smaller and diffusely distributed over the cell surface suggesting that the forces responsible for the patching the antibody-induced clusters are disrupted. Importantly also the patching of cross-linked hTfR was inhibited showing the importance of cholesterol in both patching phenomena.

Patches of GPI-anchored PLAP Accumulate src-like Tyrosine Kinase fyn

Cross-linked raft components may sequester and stabilize raft lipid domains that coalesce to become large membrane patches. This predicts that these patches are enriched in specific non–cross-linked raft membrane proteins which preferentially partition into these lipid domains. To test this we followed the distribution of non–cross-linked PLAP in cells with patched HA (and vice versa). We could occasionally demonstrate enrichment of non–cross-linked PLAP in HA patches, this behavior was however quite variable (data not shown). Possibly, movement of proteins with an extracellular domain into the patches is sterically hindered by tightly packed proteins and antibodies. To circumvent this problem we studied whether patching of

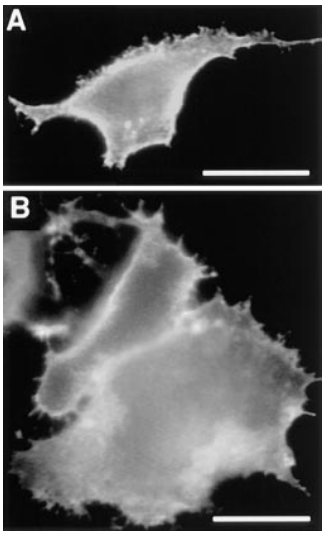

Figure 5. PLAP and hTfR patching depends on membrane cholesterol. BHK cells transiently expressing PLAP (*A*) and hTfR (*B*) were depleted of membrane cholesterol using cyclodextrin extraction. PLAP and hTfR were cross-linked using anti-PLAP and anti-hTfR mAb, respectively, followed by rhodamine-coupled secondary antibodies. Patching of PLAP as well as hTfR is inhibited under these conditions. Bar, 5 μm.

PLAP—associated to the outer leaflet of the plasma membrane via a GPI–lipid anchor—influences the distribution of raft proteins anchored in the cytoplasmic leaflet of the plasma membrane bilayer. In these experiments we studied the distribution of the src-like protein tyrosine kinase fyn, which is anchored into the cytoplasmic leaflet of the plasma membrane by two fatty acyl chains and may specifically partition into raft domains (Wolven et al., 1997). BHK cells were transfected and transiently coexpressed fyn and PLAP. Immunofluorescence after FA/MeOH fixation using anti-fyn polyclonal antibodies showed that fyn was mostly evenly distributed over the plasma membrane (Fig. 6 *A*). The morphological changes and formation of intracellular aggregates in fyn-overexpressing cells did not affect the analysis. PLAP patching was then induced at 12°C by incubation with anti-PLAP mAb and respective rhodamine labeled anti–mouse antibodies. Subsequently, the cells were fixed using FA/MeOH and the distribution of fyn was analyzed by immunofluorescence using polyclonal rabbit anti-fyn antibodies and FITC-coupled secondary antibodies. Most interestingly patching of PLAP (Fig. 6 *B*) caused a dramatic change in fyn pattern (Fig. 6 *C*) that became concentrated in domains of the plasma membrane that frequently coincided with patched PLAP (see insert Fig. 6, *B* and *C*). In control experiments the effect of TfR patching was analyzed in BHK cells coexpressing hTfR and fyn using anti-hTfR mAb for patching as described above. In most cells there was no visible effect of hTfR patching on the distribution of fyn that remained evenly distributed in the plasma membrane. Occasionally patching of hTfR induced concentration of fyn in subdomains of the plasma membrane that however did not significantly overlap with hTfR patches (data not shown).

These findings show that patches of outer leaflet-anchored PLAP attract inner leaflet components of the lipid bilayer and strongly support the notion that patches of PLAP represent specific raft lipid domains.

Coclustering of HA and PLAP Is Independent of Caveolae

We used electron microscopy to study the morphology of

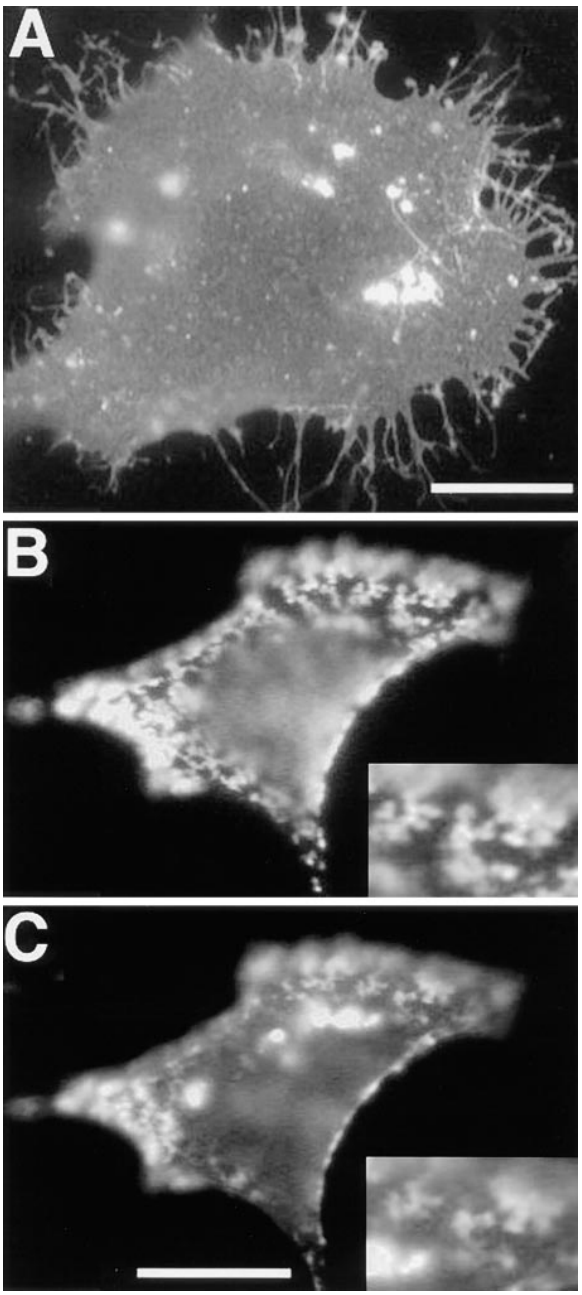

Figure 6. Accumulation of fyn in membrane domains formed by patched PLAP. *A* shows distribution of overexpressed fyn in FA/MeOH-fixed BHK cells. Patches of PLAP are shown in *B*, and the corresponding distribution of fyn in *C*. The inserts show a detail of the overlap between PLAP and fyn staining. The faint diffuse signal in the rhodamine (*PLAP*) channel that coincides with the intensely bright fyn aggregates (*FITC*) is most probably because of a small overflow from the FITC to the rhodamine channel. The overlap between the patched PLAP and the signal from the fyn immunofluorescence at the cell surface is however clearly independent from the intracellular fyn aggregates. Bars: (*A*) 10 μm; (*C*) 5 μm.

the patched membrane components. First, PLAP and TfR were coexpressed in BHK cells and copatching was performed as described above. However, now colloidal gold-labeled secondary antibodies were used to detect and cross-link the respective primary antibodies. 6-nm gold-labeled anti–mouse antibodies were used for the mouse mAb against hTfR and PLAP polyclonal rabbit antibodies were cross-linked with 12-nm gold. The relative distribution of the membrane proteins was analyzed in Epon sections of the transfected cells. The analysis confirmed the sharp segregation of PLAP and hTfR patches seen in immunofluorescence. Both patches covered large areas of the plasma membrane (>500 nm) and the transition of one domain to the other is very sharp (Fig. 7 *A*, *arrowheads*). PLAP patches are occasionally found in the vicinity of caveolar invaginations (Fig. 7 *C*, *arrowhead*) but were mostly detected at smooth domains of the plasma membrane. Importantly, hTfR patches only occasionally coincided with clathrin-coated invaginations (Fig. 7 *B*, *arrow*) in line with our interpretation that the high level of hTfR overexpression saturates the plasma membrane AP2/clathrin internalization pathway. This together with the segregation of patches of PLAP and hTfR del 5–41 shows that segregation is independent of the interaction of hTfR with clathrin-coated pits.

We then studied the copatching of two raft markers using PLAP- and HA-overexpressing cells in electron microscopy. PLAP was cross-linked with anti-PLAP mAb followed by 6-nm gold-labeled anti–mouse antibodies. 12-nm gold antibodies were used for the detection and clustering of rabbit polyclonal anti-HA antibodies. As seen in immunofluorescence the two gold particles showed extensive colocalization on the cell surface showing that movement of the independently cross-linked raft markers into closely coinciding patches can be followed at the electron-microscopical level. Copatches of HA and PLAP are mostly found at non-invaginated regions of the PM (Fig. 7, *E* and *F*, *arrow* depicts clathrin-coated invagination). Thus the copatching of HA and PLAP cannot be explained by parallel movement of the two raft markers into caveolae as described previously for coclustering of two different GPI-anchored proteins (Mayor et al., 1994).

Several reports describe a redistribution of raft markers into caveolae following cross-linking with antibodies or multivalent toxins (Mayor et al., 1994; Parton, 1994; Fujimoto, 1996) We therefore addressed not only the role of caveolae as defined by morphological criteria, but also the possible involvement of caveolin 1, a cholesterol-binding protein involved in the formation of caveolar invaginations. We performed copatching experiments in 2B2318 T–cell hybridoma cells. These cells have been shown not to express caveolin and as a consequence not to have caveolae (Fra et al., 1995). As raft markers we used GPI-anchored Thy-1 cross-linked with an mAb and GM1 cross-linked with FITC-CTx. After simultaneous incubation with anti–Thy-1 antibodies and FITC-CTx followed by further cross-linking with the rhodamine anti–mouse antibody, we observed extensive overlap of the two markers (Fig. 8). These observations demonstrate that copatching of the two membrane elements requires neither caveolin nor caveolae.

Stabilization of Membrane Domains by Antibody-induced Cross-linking

Triton X-100 insolubility has been used as a diagnostic tool to identify raft membrane proteins. We therefore asked how far detergent insolubility is related to antibody-induced patching, which we here used as an indication for

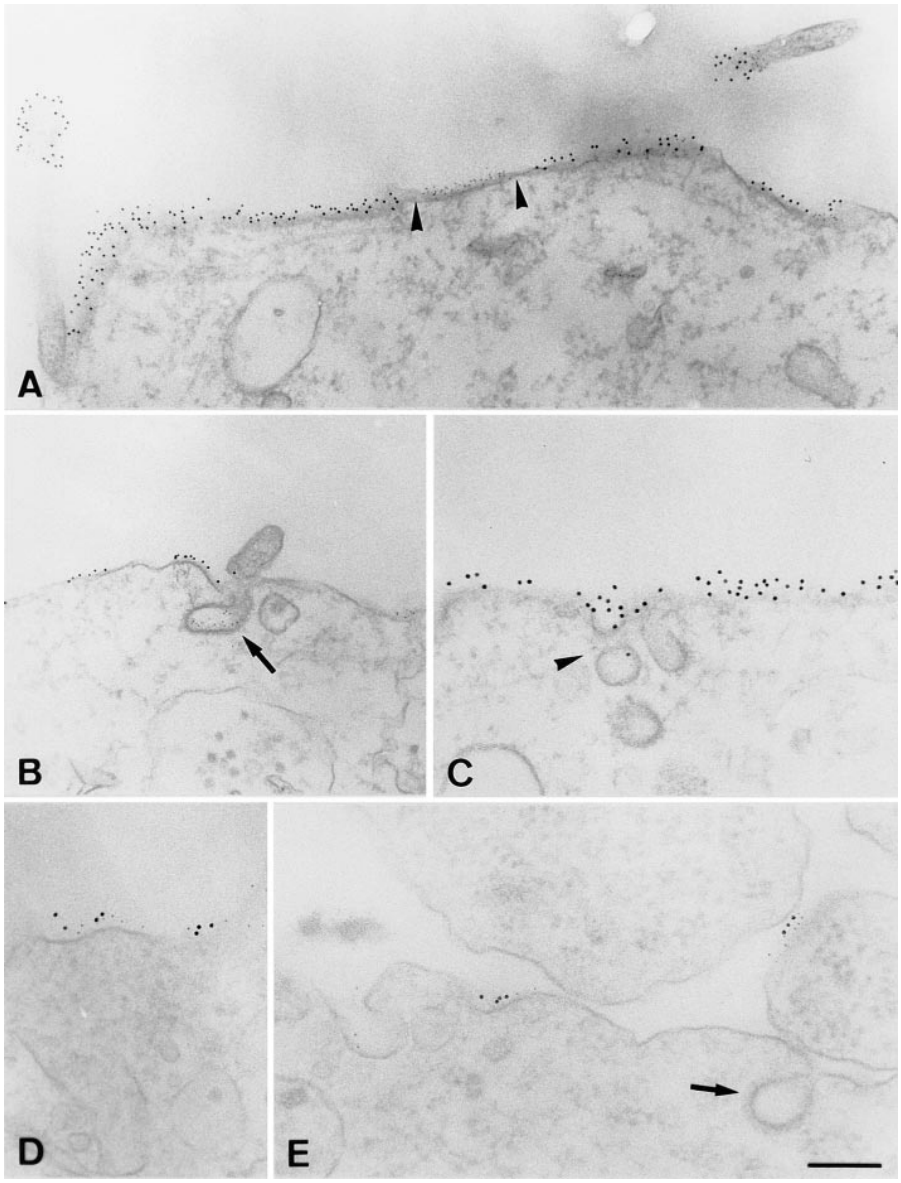

Figure 7. Electron microscopical analysis of patched membrane components. *A* and *B* show separation of PLAP patches (12-nm gold) and hTfR patches (6-nm gold). *Arrowheads*, the sharp boundaries between the patches. Arrows in *B* show a clathrin-coated invagination labeled for hTfR. *C* shows patches of PLAP surrounding caveolar-like, noncoated invaginations (*arrowhead*). *D* and *E* show copatching of HA (12-nm gold) and PLAP (6-nm gold) on smooth membrane regions. Arrow in *E* marks clathrin-coated invagination. Bars: (*A–C*) 250 nm; (*D* and *E*) 150 nM.

specific raft lipid–protein interactions. We tested whether cross-linking with antibodies had an effect on the association of PLAP to a Triton X-100–insoluble membrane fraction. We transfected cells transiently with the PLAP expression construct and cross-linked as described above with antibodies. Subsequently the cells were solubilized with 2% Triton X-100 at 4°C and subjected to flotation by a Optiprep™ density gradient centrifugation in order isolate a Triton X-100–insoluble membrane fractions. PLAP was detected after solubilization with Triton X-100 at 4°C by Western blot analysis of the gradient fractions (Fig. 9, *left*). PLAP floated to 20% Optiprep™ irrespective of whether it was cross-linked with antibodies or not. Interestingly, the yield of PLAP in the light Triton X-100–resistant membrane fraction was significantly higher if PLAP was cross-linked with antibodies. Stabilization of DIG association by antibody-induced patching became even more evident if solubilization was performed at 30°C, at which temperature uncross-linked PLAP became completely solubilized. Under these conditions a significant fraction of the patched PLAP floats with the detergent-resistant low density membranes. This protective effect was also observable if cells were cholesterol-depleted using cyclodextrin, i.e., under conditions that lead to reduction of morphologically visible copatching and to a decrease of insolubility of monomeric PLAP (not shown). This indicates that either residual cholesterol may be sufficient to produce a raft-like environment in the clusters of PLAP or that the antibody cross-linked PLAP molecules gather lipids such as glycosphingolipids independently of cholesterol and that this assembly is then protected against Triton X-100 solubilization.

We next studied the effects of cross-linking on the Triton X-100 solubility of VSV-G. Cells were infected with VSV for 2 h and then treated with cycloheximide to chase VSV-G to the cell surface. After extraction with 2% Triton X-100 at 4°C VSV-G the samples were analyzed by Optiprep™ gradient centrifugation (Fig. 9, *right*). Even though VSV-G copatches to a certain extent with PLAP it is Triton X-100 soluble and the bulk of VSV-G resided in

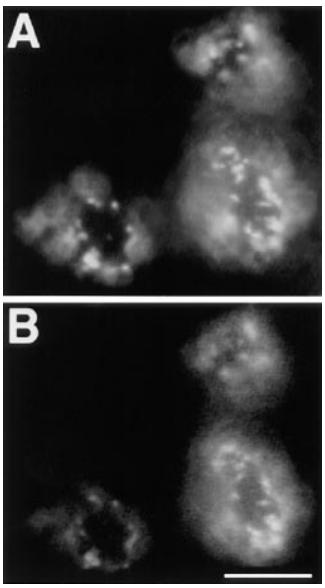

Figure 8. Copatching in T hybridoma cells. GM1 and Thy-1 copatching was induced in 2B2318 T–hybridoma cells by simultaneous incubation with anti–Thy-1 mAb and FITC-CTx followed by incubation with rhodamine anti–mouse antibodies. *A* depicts distribution Thy-1 patches and *B* distribution of the patches of GM1 CTx. Bar, 5 μm.

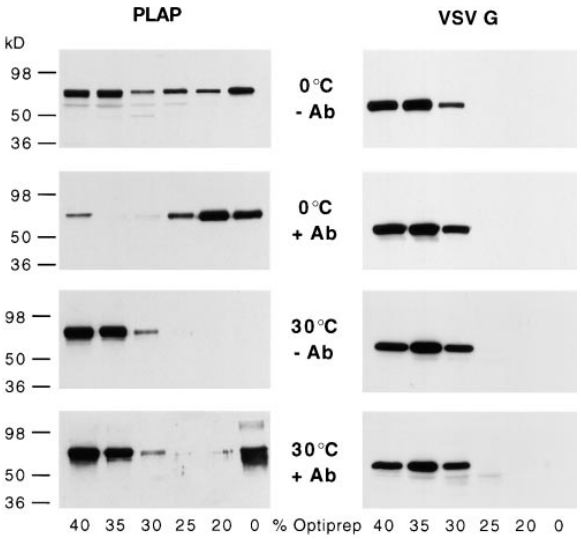

Figure 9. Stabilization of membrane domains by antibody cross-linking. BHK cells expressed PLAP after transient transfection or VSV-G introduced by VSV infection. PLAP (*left*) and VSV-G (*right*) were patched using an mAb against PLAP and polyclonal antibodies against VSV-G, respectively, followed by the respective secondary antibodies. Cells were subsequently lysed in 2% Triton X-100 at 4° or 30°C. Fractions of an Optiprep™–sucrose flotation step gradient were analyzed by Western blot using anti-PLAP and anti–VSV-G antibodies. Antibody-induced patching (+*Ab*) significantly increases the amount of PLAP associated to a Triton X-100–insoluble membrane fraction that floats to the interphase of 20% Optiprep™/10% sucrose and 0% Optiprep™/10% sucrose, whereas VSV-G remains in high density fraction irrespective whether it was cross-linked or not.

the heavy Optiprep™ fraction irrespective whether it was cross-linked with antibodies or not. Thus the lipid associated to VSV-G clusters are less tightly bound than the lipids associated to cross-linked PLAP.

Discussion

Biophysical analysis on artificial membranes have demonstrated cohesive forces between glycosphingolipids themselves and between sphingolipids and cholesterol (for review see Brown, 1998). These forces are thought to be responsible for the formation of domains in an environment of unsaturated glycerophospholipids. In cell membranes these forces are postulated to mediate a similar assembly of sphingolipid–cholesterol raft domains predicted to be in a L_o phase separated from an L_d phase of the surrounding unsaturated phosphatidylcholine (PC)-rich environment. These different liquid membrane phases have been first described in model membranes containing cholesterol and PC with saturated acyl chains (Sankaram and Thompson, 1991). Cholesterol has then been shown to trigger separation of a detergent-insoluble L_o phase from a L_d phase in sphingolipid and unsaturated PC containing model membranes i.e. to be able to generate L_o and L_d phases in mixtures of naturally occurring lipids (Ahmed et al., 1997). At high temperatures lipid bilayers have reduced tendency to form coexisting L_o and L_d phases (Sankaram and Thompson, 1991). However, the coexistence of L_o and L_d phases at 37°C could be demonstrated in artificial bilayers mimicking the lipid composition of the plasma membrane (Ahmed et al., 1997). In line with these findings, we find that at 12°C as well as at 37°C there exist specific lipid-dependent attractive or repellant forces between patched membrane components. These forces have to be attributed to properties of the respective membrane components. Our observations do not exclude that these forces cause the formation of lipid domains as a consequence of cross-linking. However, we suggest that lateral cross-linking of a membrane component causes multiplication of membrane interactions and as a consequence intrinsically existing weak interactions become exaggerated and can be detected as specific repellant and attractive forces. We observed coalescence of patched raft markers such as GPI-anchored PLAP with Influenza HA, and the raft lipid ganglioside GM1 as well as copatching of GPI-anchored Thy-1 with GM1. This suggests that copatching is a consequence of the coalescence of a common lipid microdomain containing the cross-linked raft membrane components. The patches of transferrin receptor are sharply separated from the patched raft components indicating that the lipids surrounding hTfR clusters are not miscible with raft domains.

Coalescence of Lipid Domains

Our data strongly suggest that copatching is mainly a lipid-mediated process. First, we observed extensive copatching of the raft lipid GM1 and different GPI-anchored proteins both linked via fatty acids to the outer leaflet of the plasma membrane. This and the copatching of PLAP and HA lacking a cytoplasmic tail domain shows that no direct cytoplasmic interactions are involved in the process. Active rearrangements of cellular components are most probably not involved as most experiments were performed at low temperatures. Patching of cross-linked PLAP as well as of cross-linked hTfR is inhibited by cyclodextrin extraction of cellular cholesterol. This underlines the demonstrated role of cholesterol in raft integrity (Scheiffele et al., 1997) and in a separation of L_d and L_o phases in artificial

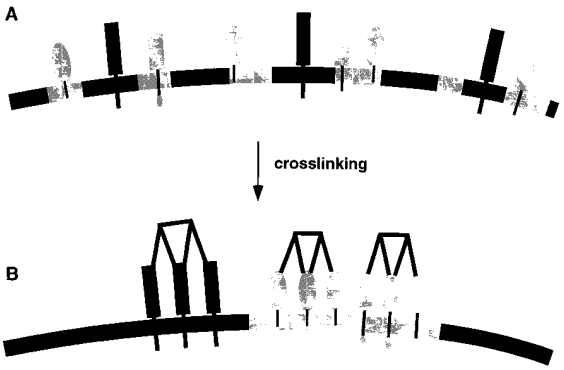

Figure 10. Bulk separation of membrane phases caused by clustering of membrane components. (*A*) Microdomains and membrane proteins in these domains are dispersed in the plasma membrane. (*B*) Cross-linking generates large and stabilized membrane domains that coalesce to form patches. If two membrane components share a preference for a lipid environment such as raft microdomains the markers will copatch into tightly associated domains. If two markers partition into different membrane environments such as raft and non-raft markers the patches will be separated.

membranes (Sankaram and Thompson, 1991; Ahmed et al., 1997) and probably in the formation of different membrane phases in which clustered hTfR and PLAP reside.

Why would cross-linking with antibodies or toxins induce patching? Lateral cross-linking of membrane proteins or lipids causes multimerization of their membrane binding sites. If the monomeric membrane component has a preference for specific membrane microdomains multiple membrane interactions of the clustered constituents will cooperatively strengthen the association. In cellular membranes this may cause an accumulation of the lipid domains around the clusters. Therefore the clusters may have a stabilizing effect on raft lipid domains themselves and on the association of the cross-linked raft marker with these domains. Indeed, we found that cross-linking of GPI-anchored PLAP with antibodies stabilizes its association with the DIG fraction, leading to increased temperature resistance to Triton X-100 solubilization. Stabilized lipid membrane domains may coalesce which leads to copatching of two clustered membrane components preferring the same lipid environment. On the other hand patched membrane components with different lipid preferences are separated (Fig. 10). We therefore suggest that the copatching of the raft markers described here is the consequence of a shared preference for raft lipids.

Different Affinities for Raft Association

An important parameter governing raft dynamics is the specific partition coefficient which can be expected to determine the raft-associated fraction of all membrane proteins and lipids. Partial copatching of cross-linked LDL-R and to an even larger extent of VSV-G indeed indicates that certain proteins exhibit a weak but significant raft interaction which is not detectable by the DIG criterion. Upon multimerization these weak interactions are strengthened and lead to formation of a raft lipid environment. The association of VSV-G to these domains is however not strong enough to confer DIG association. Therefore probably only proteins which strongly interact with rafts are Triton X-100 insoluble, whereas weakly raft-associated proteins (for example VSV-G) are Triton X-100 soluble. Tightly packed VSV-G in the budding virus may therefore weakly interact with raft domains and cause formation of microdomains and indeed VSV envelopes have been shown to be somewhat enriched in sphingomyelin and cholesterol, compared with the host plasma membrane (Welti and Glaser, 1994). Sequestration of raft lipid domains by viral proteins may also explain a phenomenon that has puzzled virologists for years namely that VSV particles specifically include antibody cross-linked GPI-anchored Thy-1 while excluding other plasma membrane proteins (Calafat et al., 1983).

Cellular Structures Regulating Raft Dynamics

Raft dynamics can be influenced by specific proteins. A good example are the caveolae (flask-shaped invaginations of the plasma membrane; see Lisanti et al., 1995; Parton, 1996). Caveolin proteins are essential components of caveolae. These proteins form large oligomers and, as demonstrated for caveolin 1, avidly bind cholesterol (Murata et al., 1995). These properties together with multiple palmitoylation could enable caveolins to sequester raft lipids and to eventually form and organize large stabilized raft domains (Dietzen et al., 1995; Monier et al., 1996). Raft markers such as gangliosides, sphingomyelin, and GPI-anchored proteins have been shown move into caveolae if cross-linked laterally with antibodies or multivalent toxins (Mayor et al., 1994; Parton, 1994; Fujimoto, 1996). Interestingly, copatching of two GPI-anchored proteins in caveolae has also been observed (Mayor et al., 1994). Like the copatching of cross-linked raft markers this phenomenon may be driven by the coalescence of stabilized raft lipid domains. The caveolae may function as traps for these clustered microdomains. However, if the size of the patched regions become too large, then their entry into caveolae is restricted.

The asymmetric lipid distribution of the apical and basolateral plasma membrane domains in polarized cells is established by a polarized delivery of transport vesicles with distinct lipid and protein composition (Weimbs et al., 1997; Keller and Simons, 1998*b*). Tight junctions inhibit lateral exchange between these membrane domains. The specific enrichment of glycolipids and raft protein markers suggests that the apical membrane is a percolating raft domain (see below) whereas the basolateral membrane is depleted of rafts and enriched in PC. In other cells such as osteoclasts, segregation of apical and basolateral markers is visible without tight junctions (Salo et al., 1996). In these cells, distinct transport vesicles may fuse with different domains of the plasma membrane and lateral diffusion is reduced possibly by extracellular matrix interactions or cytoskeletal structures.

Lateral cross-linking may play a role in the generation of patches of clustered rafts in intracellular membranes. This may be accomplished by adaptors which accumulate specific proteins or by intracellular lectins such as VIP 36 that may laterally cross-link glycosylated molecules (Fiedler et al., 1994). Such mechanisms can generate subdomains in

intracellular membranes and be an important element of intracellular sorting mechanisms.

Raft Dispersion and Cellular Responses to Patching

Here we suggest that rafts at steady state are small and highly dispersed in line with theoretical considerations (Vaz and Almeida, 1993). When the dispersed raft domains are induced to form patches by clustering of membrane components they coalesce into percolating large domains. These changes in the structure of raft domains may represent an important starting point for the generation of intracellular signals. According to this view, raft-associated signaling molecules are normally separated in dispersed non-percolating raft domains. In the large raft domains formed by patching these molecules come together and can interact with each other and their targets (see discussion in Vaz and Almeida, 1993). This is supported by our finding that patches of PLAP an outer leaflet GPI-anchored protein accumulate intracellular src-related protein tyrosine kinase fyn, which is anchored via double fatty acylation to the inner leaflet of the lipid bilayer (Shenoy-Scaria et al., 1994; Wolven et al., 1997). Specific interactions between outer leaflet raft lipids and the inner leaflet lipids may mediate a coupling between the two leaflets of the bilayer in raft domains. Possibly these interactions involve intercalation of outer leaflet lipid acyl chains into the inner leaflet and vice versa or may involve transbilayer cholesterol dimers (Harris et al., 1995). Binding could also be mediated by other membrane proteins which serve as receptors for fyn. The data presented here suggest a mechanism of signal transduction mediated by cross-linking of GPI-anchored proteins (Brown, 1993) and strongly support a role for raft lipid domains in the activation of doubly acylated src-like protein tyrosine kinases.

Several cellular responses have been described after patching of membrane components, for example, nonclathrin–mediated endocytic events (Deckert et al., 1996) or activation of T-lymphocytes (Brown, 1993). Patches of cross-linked membrane components were moreover described to move in an actin-dependent manner to one pole of lymphocytes in a process called capping. Interestingly, the involvement of lipid domains in this process was suggested in early studies (Karnovsky et al., 1982) supported by the finding that cholesterol depletion inhibited capping (Hoover et al., 1983). These studies however did not describe an effect of cholesterol depletion on the actin-independent patching phenomenon. We suggest that this process involves coalescence of lipid microdomains leading to a copatching of small cross-linked entities with one another. Cross-linking of the IgE receptor FcεRI by multimeric antigens is a well-studied example (for review see Holowka and Baird, 1996). This cross-linking induces the formation of lateral assemblies of FcεRI receptors, which in mast and basophilic cells mediate an allergic response such as secretion of histamines. At the sites of clustered IgE receptors, specific lipid domains were shown to form that could be specifically stained with lipid dye DiI16 (Thomas et al., 1994). The fraction of FcεRI which was found in a Triton X-100–resistant membrane fraction (using very low amounts of detergent) as well as the amount of DIG-associated tyrosine kinase lyn increased (Field et al., 1997). Moreover antibody cross-linked ganglioside G1b copatched with clustered FcεRI receptors (Pierini et al., 1996). Therefore the domains of patched FcεRI are very similar to the domains of clustered raft proteins and lipids that we describe here. Our data presented here support the view that the formation of specific raft lipid domains at the sites of patched FcεRI are important for the signaling cascade after FcεRI engagement.

The generation of stabilized membrane lipid domains from a highly dispersed distribution by cross-linking of membrane components may represent a general mode of regulating membrane structure. Interaction with intracellular (adaptors and coats) or extracellular ligands (multimeric antigens binding to IgE) will distribute proteins into patches that in turn recruit downstream effector molecules. Cooperativity ensures specificity and the regulation of the process. This lipid-mediated mechanism may play a role for different functions of the cell ranging from intracellular membrane sorting to signaling processes.

We gratefully acknowledge Drs. D. Brown, M. Roth, K. Matter, and G. Alonso for the generous gifts of cDNA constructs and antibodies. We thank E. Levi for her help in constructing and analyzing expression constructs, and T. Hyman for critically reading the manuscript. We moreover thank the participants of the 16 October 1997 EMBL Cell Biology Seminar for constructive criticism. The Simons lab helped with stimulating discussions throughout the work.

T. Harder is supported by a Deutsche Forschurgsgemeinschaft research fellowship.

Received for publication 4 November 1997 and in revised form 2 April 1998.

References

Ahmed, S.N., D.A. Brown, and E. London. 1997. On the origin of sphingolipid/cholesterol-rich detergent-insoluble cell membranes: physiological concentrations of cholesterol and sphingolipid induce formation of a detergent insoluble, liquid ordered lipid phase in model membranes. *Biochemistry.* 36: 10944–10953.

Blackman, M.A., F.E. Lund, S. Surman, R.B. Corley, and D.L. Woodland. 1992. Major histocompatibility complex restricted recognition of retroviral superantigens by V β 17+ T cells. *J. Exp. Med.* 176:275–280.

Brewer, C.B., and M.G. Roth. 1991. A single amino acid change in the cytoplasmic domain alters the polarized delivery of influenza virus hemagglutinin. *J. Cell Biol.* 114:413–421.

Brown, D.A. 1992. Interactions between GPI-anchored proteins and membrane lipids. *Trends Cell Biol.* 2:338–343.

Brown, D.A. 1993. The tyrosine kinase connection: how GPI-anchored proteins activate T cells. *Curr. Opin. Immunol.* 5:349–354.

Brown, D.A., and J.K. Rose. 1992. Sorting of GPI-anchored proteins to glycolipid-enriched membrane subdomains during transport to the cell surface. *Cell.* 68:533–544.

Brown, D.A., B. Crise, and J.K. Rose. 1989. Mechanism of membrane anchoring affects polarized expression of two proteins in MDCK cells. *Science.* 245: 1499–1501.

Brown, R.E. 1998. Sphingolipid organisation in biomembranes: what physical studies of model membranes reveal. *J. Cell Sci.* 111:1–9.

Calafat, J., H. Janssen, P. Demant, J. Hilgers, and J. Zavada. 1983. Specific selection of host cell glycoproteins during assembly of murine leukaemia virus and vesicular stomatitis virus: presence of Thy-I glycoprotein and absence of H-2, Pgp1 and T-200 glycoproteins on the envelopes of these virus particles. *J. Gen. Virol.* 64:1241–1253.

Cerneus, D.P., E. Ueffing, G. Posthuma, G.J. Strous, and A. van der Ende. 1993. Detergent insolubility of alkaline phosphatase during biosynthetic transport and endocytosis. Role of cholesterol. *J. Biol Chem.* 268:3150–3155.

Deckert, M., M. Ticchioni, and A. Bernard. 1996. Endocytosis of GPI-anchored proteins in human lymphocytes: Role of glycolipid-based domains, actin cytoskeleton, and protein kinases. *J. Cell Biol.* 133:791–799.

Dietzen, D.J., W.R. Hastings, and D.M. Lublin. 1995. Caveolin is palmitoylated on multiple cysteine residues: Palmitoylation is not required for localization of caveolin to caveolae. *J. Biol. Chem.* 270:6838–6842.

Fiedler, K., R.G. Parton, R. Kellner, T. Etzold, and K. Simons. 1994. VIP36, a novel component of glycolipid rafts and exocytic carrier vesicles in epithelial cells. *EMBO (Eur. Mol. Biol. Organ.) J.* 13:1729–1740.

Field, K.A., D. Holowka, and B. Baird. 1997. Compartmentalized activation of the high affinity immunoglobulin E receptor within membrane domains. *J. Biol. Chem.* 272:4276–4280.

Fra, A.M., E. Williamson, K. Simons, and R.G. Parton. 1995. De novo formation of caveolae in lymphocytes by expression of VIP21-caveolin. *Proc. Natl. Acad. Sci. USA*. 92:8655–8659.

Fujimoto, T. 1996. GPI-anchored proteins, glycosphingolipids, and sphingomyelin are sequestered to caveolae only after crosslinking. *J. Histochem. Cytochem.* 44:929–941.

Hanada, K., M. Nishijima, Y. Akamatsu, and R.E. Pagano. 1995. Both sphingolipids and cholesterol participate in the detergent insolubility of alkaline phosphatase, a glycosylphosphatidylinositol-anchored protein, in mammalian membranes. *J. Biol. Chem.* 270:6254–6260.

Harder, T., and V. Gerke. 1993. The subcellular distribution of early endosomes is affected by the annexin II_2p11_2 complex. *J. Cell Biol.* 123:1119–1132.

Harder, T., and K. Simons. 1997. Caveolae, DIGs, and the dynamics of sphingolipid-cholesterol microdomains. *Curr. Opin. Cell Biol.* 9:534–542.

Harris, J.S., D.E. Epps, S.R. Davio, and F.J. Kezdy. 1995. Evidence for transbilayer, tail-to-tail cholesterol dimers in dipalmitoylglycerophosphocholine liposomes. *Biochemistry.* 34:3851–3857.

Hirao, M., N. Sato, T. Kondo, S. Yonemura, M. Monden, T. Sasaki, Y. Takai, S. Tsukita, and S. Tsukita. 1996. Regulation mechanism of ERM protein/plasma membrane association: possible involvement of phosphatidyl inositol turnover and rho-dependent signaling pathway. *J. Cell Biol.* 135:37–52.

Holowka, D., and B. Baird. 1996. Antigen-mediated IgE receptor aggregation and signaling: a window on cell surface structure and dynamics. *Ann. Rev. Biophys. Biomol. Struct.* 25:79–112.

Hoover, R.L., E.A. Dawidowicz, J.M. Robinson, and M.J. Karnovsiky. 1983. Role of cholesterol in the capping of surface immunoglobulin receptors on murine lymphocytes. *J. Cell Biol.* 97:73–80.

Ikonen, E., M. Tagaya, O. Ullrich, C. Montecucco, and K. Simons. 1995. Different requirements for NSF, SNAP, and Rab proteins in apical and basolateral transport in MDCK cells. *Cell.* 81:571–580.

Karnovsky, M.J., A.M. Kleinfeld, R.L. Hoover, and R.D. Klausner. 1982. The concept of lipid domains in membranes. *J. Cell Biol.* 94:1–6.

Keller, P., and K. Simons. 1998*a*. Cholesterol is required for surface transport of Influenza virus hemagglutinin. *J. Cell Biol.* 140:1357–1367.

Keller, P., and K. Simons. 1998*b*. Post-Golgi biosynthetic trafficking. *J. Cell Sci.* 110:3001–3009.

Klein, U., G. Gimpl, and F. Fahrenholz. 1995. Alteration of the myometrial plasma membrane cholesterol content with β-cyclodextrin modulates the binding affinity of the oxytocin receptor. *Biochemistry.* 34:13784–13793.

Kreis, T.E. 1986. Microinjected antibodies against the cytoplasmic domain of vesicular stomatitis virus glycoprotein block its transport to the cell surface. *EMBO (Eur. Mol. Biol. Organ.) J.* 5:931–941.

Kurzchalia, T.V., E. Hartmann, and P. Dupree. 1995. Guilt by insolubility—does a protein's detergent insolubility reflect caveolar location? *Trends Cell Biol.* 5:187–189.

Lazarovits, J., and M. Roth. 1988. A single amino acid change in the cytoplasmic domain allows the influenza virus haemagglutinin to be endocytosed through coated pits. *Cell.* 53:743–752.

Lisanti, P.L., P.E. Scherer, Z. Tang, E. Kübler, A.J. Koleske, and M. Sargiacomo. 1995. Caveolae and human disease: functional roles in transcytosis, potocytosis, signalling, and cell polarity. *Semin. Dev. Biol.* 6:47–58.

Matter, K., and I. Mellman. 1994. Mechanisms of cell polarity: sorting and transport in epithelial cells. *Curr. Opin. Cell Biol.* 6:545–554.

Matter, K., W. Hunziker, and I. Mellman. 1992. Basolateral sorting of LDL receptor in MDCK cells: the cytoplasmic domain contains two tyrosine-dependent targeting determinants. *Cell.* 71:741–753.

Mayor, S., and F.R. Maxfield. 1995. Insolubility and redistribution of GPI-anchored proteins at the cell surface after detergent treatment. *Mol. Biol. Cell.* 6:929–944.

Mayor, S., K.G. Rothberg, and F.R. Maxfield. 1994. Sequestration of GPI-anchored proteins in caveolae triggered by cross-linking. *Science.* 264:1948–1951.

Merrit, E.A., S. Sarfaty, F. van den Akker, C. L'Hoir, J.A. Martial, and W.G.J. Hol. 1994. Crystal structure of cholera toxin B-pentamer bound to receptor GM1 pentasaccharide. *Protein Science.* 3:166–175.

Monier, S., D.J. Dietzen, W.R. Hastings, D.M. Lublin, and T.V. Kurzchalia. 1996. Oligomerisation of VIP21-caveolin in vitro is stabilized by long chain fatty acylation or cholesterol. *FEBS (Fed. Eur. Biochem. Soc.) Lett.* 388: 143–149.

Mumby, S.M. 1997. Reversible palmitoylation of signaling proteins. *Curr. Opin. Cell Biol.* 9:148–154.

Murata, M., J. Peranen, R. Schreiner, F. Wieland, T.V. Kurzchalia, and K. Simons. 1995. VIP21/caveolin is a cholesterol-binding protein. *Proc. Natl. Acad. Sci. USA*. 92:10339–10343.

Müsch, A., H. Xu, D. Shields, and E. Rodriguez-Boulan. 1996. Transport of vesicular stomatitis virus G-protein to the cell surface is signal mediated in polarized and nonpolarized cells. *J. Cell Biol.* 133:543–558.

Odorizzi, G., and I.S. Trowbridge. 1997. Structural requirements for basolateral sorting of the human transferrin receptor in the biosynthetic and endocytic pathways of Madin-Darby canine kidney cells. *J. Cell Biol.* 137:1255–1264.

Osborn, M., N. Johnsson, J. Wehland, and K. Weber. 1988. The submembraneous location of p11 and its interaction with the p36 substrate of pp60 src kinase *in situ*. *Exp. Cell Res.* 175:81–96.

Parton, R.G. 1994. Ultrastructural localization of gangliosides; GM1 is concentrated in caveolae. *J. Histochem. Cytochem.* 42:155–166.

Parton, R.G. 1996. Caveolae and caveolins. *Curr. Opin. Cell Biol.* 8:542–548.

Parton, R.G., and K. Simons. 1995. Digging into caveolae. *Science.* 269:1398–1399.

Pierini, L., D. Holowka, and B. Baird. 1996. Fc epsilon RI-mediated association of 6-micron beads with RBL-2H3 mast cells results in exclusion of signaling proteins from the forming phagosome and abrogation of normal downstream signaling. *J. Cell Biol.* 134:1427–1439.

Rodgers, W., B. Crise, and J.K. Rose. 1994. Signals determining protein tyrosine kinase and glycosyl-phosphatidyl-anchored protein targeting to a glycolipid-enriched membrane fraction. *Mol. Cell. Biol.* 14:5384–5391.

Rodriguez-Boulan, E., and W.J. Nelson. 1989. Morphogenesis of the polarized epithelial cell phenotype. *Science.* 245:718–725.

Roth, M.G., and P.C. Sternweis. 1997. The role of lipid signaling in constitutive membrane transport. *Curr. Opin. Cell Biol.* 9:519–526.

Salo, J., K. Metsikkö, H. Palokangas, P. Lehenkari, and H.K. Väänänen. 1996. Bone-resorbing osteoclasts reveal a dynamic division of basal plasma membrane into two different domains. *J. Cell Sci.* 109:301–307.

Sankaram, M.B., and T.E. Thompson. 1991. Cholesterol-induced fluid-phase immiscibility in membranes. *Proc. Natl. Acad. Sci. USA*. 88:8686–8690.

Scheiffele, P., M.G. Roth, and K. Simons. 1997. Interaction of influenza virus hemagglutinin with sphingolipid-cholesterol membrane domains via its transmembrane domains. *EMBO (Eur. Mol. Biol. Organ.) J.* 16:5501–5508.

Schroeder, R., E. London, and D. Brown. 1994. Interactions between saturated acyl chains confer detergent resistance to lipids and glycosylphosphatidylinositol (GPI)-anchored proteins: GPI-anchored proteins in liposomes and cells show similar behavior. *Proc. Natl. Acad. Sci. USA*. 91:12130–12134.

Shenoy-Scaria, A.M., D.J. Dietzen, J. Kwong, D.C. Link, and D.M. Lublin. 1994. Cysteine(3) of Src family protein tyrosine kinases determines palmitoylation and localization in caveolae. *J. Cell Biol.* 126:353–363.

Simons, K., and E. Ikonen. 1997. Sphingolipid-cholesterol rafts in membrane trafficking and signalling. *Nature.* 387:569–572.

Skibbens, J.E., M.G. Roth, and K.S. Matlin. 1989. Differential extractability of influenza virus hemagglutinin during intracellular transport in polarized epithelial cells and nonpolar fibroblasts. *J. Cell Biol.* 108:821–832.

Spiegel, S., S. Kassis, M. Wilchek, and P.H. Fishman. 1984. Direct visualization of redistribution and capping of fluorescent gangliosides on lymphocytes. *J. Cell Biol.* 99:1575–1581.

Thomas, J.L., D. Holowka, B. Baird, and W.W. Webb. 1994. Large-scale co-aggregation of fluorescent lipid probes with cell surface proteins. *J. Cell Biol.* 125: 795–802.

Vaz, W.L., and P.F. Almeida. 1993. Phase topology and percolation in multiphase bilayers: is the biological membrane a domain mosaic? *Curr. Opin. Struct. Biol.* 3:482–488.

Wandinger-Ness, A., M.K. Bennet, C. Antony, and K. Simons. 1990. Distinct transport vesicles mediate the delivery of plasma membrane proteins to the apical and basolateral domains of MDCK cells. *J. Cell Biol.* 111:987–1000.

Warren, R.A., F.A. Green, and C.A. Enns. 1997. Saturation of the endocytic pathway for the transferrin receptor does not affect the endocytosis of the epidermal growth factor receptor. *J. Biol. Chem.* 272:2116–2121.

Weimbs, T., S.H. Low, S.J. Chapin, and K. Mostov. 1997. Apical targeting in polarised cells: there's more afloat than rafts. *Trends Cell Biol.* 7:393–399.

Welti, R., and M. Glaser. 1994. Lipid domains in model and biological membranes. *Chem. Phys. Lipids.* 73:121–137.

Wolven, A., H. Okamura, Y. Rosenblatt, and M.D. Resh. 1997. Pamitoylation of p59fyn is reversible and sufficient for plasma membrane association. *Mol. Biol. Cell.* 8:1159–1173.

Yoshimori, T., P. Keller, G.M. Roth, and K. Simons. 1996. Different biosynthetic transport routes to the plasma membrane in BHK and CHO cells. *J. Cell Biol.* 133:247–256.